

See discussions, stats, and author profiles for this publication at: <https://www.researchgate.net/publication/272142784>

Selective Electrophoretic Deposition of CdSe Nanoplatelets

ARTICLE *in* CHEMISTRY OF MATERIALS · AUGUST 2014

Impact Factor: 8.35 · DOI: 10.1021/cm501713s

CITATIONS

2

READS

11

4 AUTHORS, INCLUDING:



[Emmanuel Lhuillier](#)
Pierre and Marie Curie University - Paris 6
48 PUBLICATIONS 294 CITATIONS

[SEE PROFILE](#)



[Sandrine Ithurria](#)
École Supérieure de Physique et de Chimie In...
34 PUBLICATIONS 744 CITATIONS

[SEE PROFILE](#)

Selective Electrophoretic Deposition of CdSe Nanoplatelets

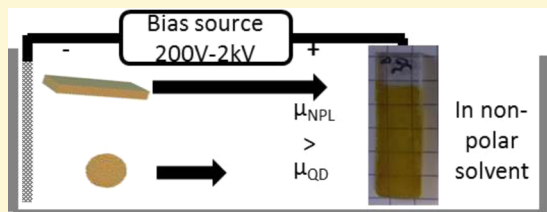
Emmanuel Lhuillier,[†] Patrick Hease,[‡] Sandrine Ithurria,[‡] and Benoit Dubertret^{*,‡}

[†]Nexdot, 10 rue Vauquelin, 75005 Paris, France

[‡]Laboratoire de Physique et d'Etude des Matériaux, ESPCI 10 rue Vauquelin, 75231 Paris, France

Supporting Information

ABSTRACT: In the fields of nanoparticle synthesis and application, the control of the particle size, shape and composition is crucial. The tuning of these different parameters can be performed during the synthesis, but often, additional selection steps to improve the purity of a given nanoparticles' population are necessary. These additional postsynthesis selection steps, that can include size selective precipitation, ultracentrifugation or liquid chromatography, are usually long and not well suited for a large quantity of materials. Here, we demonstrate that electrophoresis performed directly in organic solvent can be used to select and/or separate semiconductor nanoparticles according to their size and shape. In particular, we show that 2D nanoplatelets (NPL) can be very efficiently separated from spherical nanoparticles as the side product obtained during the NPL synthesis. The selectivity of the electrophoretic deposition we observe is mostly related to the nanoparticle surface charge. We show that centimeter scale, uniform film of nanoplatelets can be obtained even on nonconducting substrates. Compared to other methods this technique is fast, easy to implement and scalable, and should find various uses both in the fields of the nanoparticle synthesis and their applications.



INTRODUCTION

The success of colloidal inorganic nanoparticles is in large part due to the ability to synthesize them with varying composition,¹ size,² shape³ and surface chemistry.⁴ In spite of the continuous progresses done in the field of nanoparticles synthesis, additional purification or selection steps are often required when nanoparticles with precise sizes, shapes, or compositions are desired. For example, in the case of quantum dots, the size, the shape, and the composition of the semiconductor nanoparticles have strong influences on their optical or electrical properties, and pure populations often mean better ensemble properties. Several postsynthetic purification methods have been developed. One of the first ones is selective precipitation.⁵ Although this technique can give a population with an exquisite control of the nanoparticle size and shape, it is time-consuming and limited to small quantities of nanoparticles. Ultracentrifugation⁶ has also been used to select nanoparticles with different sedimentation coefficients in a density gradient, but apart from a few examples,^{7,8} this technique is mostly limited to water-soluble nanoparticles. In addition, the recovery of the different fractions after the centrifugation is not easy and often involves puncture of the tubes. Liquid chromatography has also been used using both high pressure⁹ and low pressure,¹⁰ with nanoparticles that have either hydrophobic¹¹ or hydrophilic^{12,13} surfaces, but the columns are easily polluted and tend to be clogged with the nanoparticles that have labile ligands. Gel electrophoresis^{14,15} has also been used as a postsynthetic sorting technique, but it can be used only with water-soluble nanoparticles. There is a need for a technique that could sort nanoparticles suspended in a non-polar solvent (preferably without the use of a support such as a gel or a chromatographic column) and that is both rapid and easily

scalable. Electrophoresis shows great promise toward fulfilling these requirements.

Electrophoresis of nanoparticles in non-polar or slightly polar solvents has been recently used as a deposition method to obtain homogeneous films of nanoparticles with controlled thickness.^{16,17} It is becoming a technique of interest for the assembly of devices such as LEDs,¹⁸ or solar cells^{19,20} or for the extraction of nanoparticles from their solvent after synthesis.²¹ From a film deposition perspective, the electrophoretic process offers a fast deposition and allows a large range of final thickness (from 10 nm to 10 μm). This method also offers the key advantage of considerably limiting the waste of material compared to spin coating, while keeping good film homogeneity. Recently, the application of electrophoretic deposition (ED) has been extended to the deposition of anisotropic particles with a controlled orientation on the electrode.²² A recent review has been proposed by Dickerson et al.²³ In spite of this recent progress the mechanism of ED remains unclear since even the electrodes on which cadmium chalcogenides nanocrystals get deposited seem to be dependent from experiment to experiment^{21,23}.

Among the nanocrystal family, 2D nanoplatelets²⁴ (NPL) are offering exceptional optical properties thanks to their atomically controlled thickness. This results in a narrow full width at half-maximum (fwhm) of the photoluminescence (PL) emission, typically around the thermal energy, and well-defined electronic transitions.²⁵ Such materials, which can be called nanoplatelets (NPL), nanosheets,²⁶ nanoribbons,²⁷ quantum belts²⁸ or

Received: May 12, 2014

Revised: June 10, 2014

Published: July 15, 2014

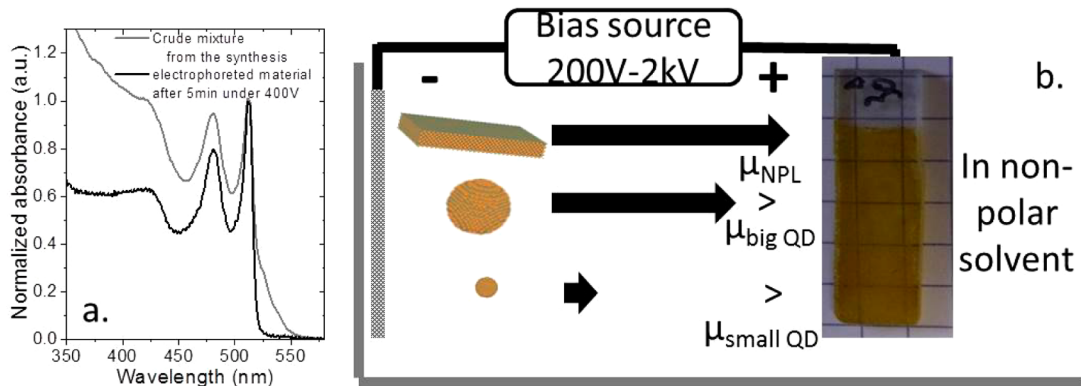


Figure 1. (a) Absorption spectrum of the crude mixture resulting from a NPL synthesis before and after electrophoresis. (b) Scheme of the electrophoretic setup.

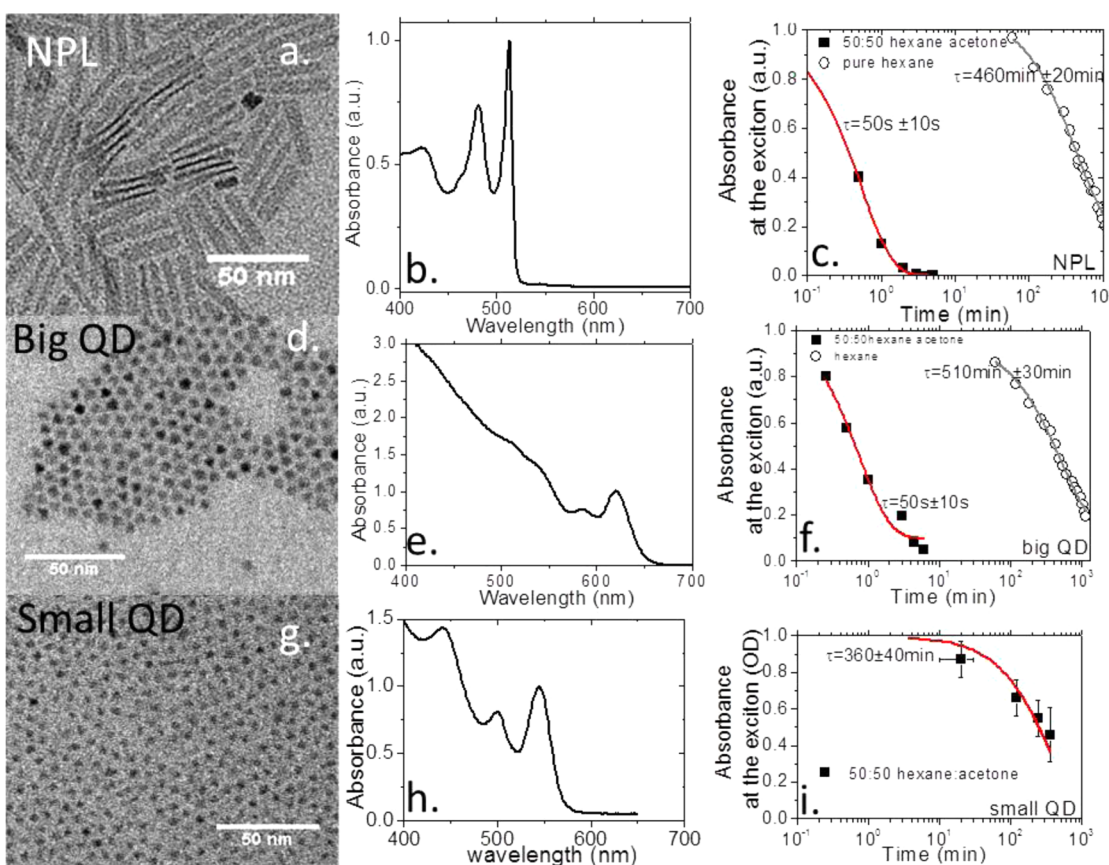


Figure 2. (a,b,c) Respectively are TEM image, absorption spectrum, and kinetic studies (i.e., absorption at the first exciton as a function of time) for CdSe NPL. (d,e,f) The same as (a,b,c) for CdSe big QD. (g,h,i) The same as (a,b,c) for CdSe small QD.

nanodisks,²⁹ depending on their shape and lateral extension,³⁰ can be grown with most cadmium chalcogenides. In addition to narrow excitonic features the spectroscopic properties of NPLs have fast PL lifetimes.³¹ Moreover this material has a strong potential from a transport point of view and we recently demonstrated *n*-type conduction using solid electrolyte gated field effect transistors.^{32,33} The colloidal growth of these 2D colloidal nanoparticles relies on the anisotropic extension of a seed thanks to the presence of two sizes of carboxylic acid used as ligands. The synthesis of NPLs is now well established, but 2D NPLs generally come with some byproducts such as other populations of NPLs and/or spherical quantum dots (QD), see Figure 1a. Among the steps toward the industrial use of the NPL,

the development of an efficient scalable method for their cleaning still needs to be developed. Here we demonstrate that ED is very efficient to select nanoparticles with different shapes and can be used as a fast large-scale method to sort NPLs. We also address the film deposition of NPLs using electrophoretic procedure.

■ EXPERIMENTAL SECTION

NPL Synthesis CdSe 510. The nanoplatelets are made using a slightly modified procedure described previously in ref 24. Briefly in a 250 mL three-neck flask, 0.96 g of Cd(OAc)₂(H₂O)₂, 3 g of oleic acid and 90 mL of octadecene (ODE) are degassed under vacuum for 30 min at 80 °C and then for 30 min at 110 °C. The flask is then cooled down, and a

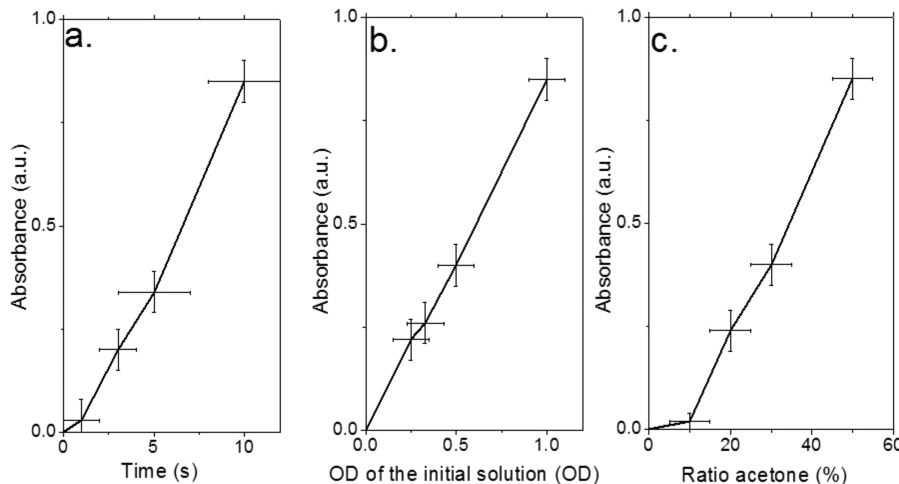


Figure 3. Evolution of the thickness of the film of NPL made by electrophoresis as a function of the time (a - applied bias is 400 V, ratio acetone 50% and deposition time is 10 s), initial concentration of particle (b - applied bias is 400 V, ratio acetone 50% and OD at the exciton peak is 1), acetone ratio (c - applied bias is 400 V, deposition time 10 s and OD at the exciton peak is 1).

mixture of 144 mg of Se in 2 mL of ODE is added to the flask. Under Ar the temperature is set at 240 °C. Once the temperature reaches 200 °C, 0.48 g of Cd(OAc)₂(H₂O)₂ is quickly added. The reaction is then performed for 40 min at 240 °C. The reaction is quenched by adding 2 mL of oleic acid. Then the particles are precipitated by adding a similar volume of ethanol. After centrifugation (5 min at 5000 rpm) the supernatant is discarded, and the solid pellet is redispersed in fresh hexane. The procedure is repeated at least three times. The optical spectra exhibits a first excitonic feature at 510 nm, see Figure 1a and Figure 2b. The obtained materials are rectangular-shaped NPL with lateral dimension of 10 nm × 40 nm, see Figure 2a.

Big QD CdSe Synthesis. In a 100 mL three-neck flask, 170 mg of Cd(Myr)₂ and 7.5 mL of ODE are stirred under vacuum at room temperature for 30 min. Meanwhile 24 mg of Se are mixed with 2 mL of ODE. Under argon atmosphere at 240 °C, 1 mL of the Se solution is quickly injected. The reaction is performed for 5 min, 0.2 mL of oleic acid is added, and then the temperature is set at 260 °C. Two mL of oleylamine are added, and the reaction is continued for 10 min. Then a mixture of 2 mL of cadmium oleate (0.5 M) and 10 mL of Se ODE (0.1 M) is prepared and then injected dropwise over 70 min. The flask is cooled down, and the nanoparticles are cleaned using ethanol as polar solvent and hexane as nonpolar solvent. The particles show a first excitonic feature around 630 nm, see Figure 2d and e.

Small QD CdSe Synthesis. The QD synthesis used follows a procedure by the Cao's group.³⁴ In a 100 mL three-neck flask, 174 mg of Cd(Myr)₂, 12 mg of Se, and 16 mL of ODE are stirred under vacuum for 30 min at room temperature. Under Ar the temperature is set at 240 °C and the reaction performed for 10 min. Then 1 mL of oleic acid is added to quench the reaction, and the flask is cooled down to room temperature. The cleaning procedure is similar to the one used for the NPL. The final particles are spherical and show an excitonic feature at 543 nm, Figure 2g and h. Small QDs with a feature at 530 nm have also been tested and lead to a similar result, see Figure 4.

NPL Synthesis CdSe 460. The CdSe nanoplatelets with an exciton peak at 460 nm are made using a procedure inspired by ref 35. In a 100 mL three-neck flask, 30 mL of ODE is degassed at room temperature for 30 min. In a vial 0.19 g of Cd(OAc)₂(H₂O)₂, 2 mL of ethanol, and 2 mL of butanol are mixed with 6 mL of Se:ODE (0.1 M) and 100 μL of oleic acid.

After stirring, this solution is introduced into a 10 mL syringe. The atmosphere is switched to Ar, and the temperature is set to 220 °C. The contents in the syringe are injected dropwise over 5 min into the flask at 220 °C. After 1 min of reaction, the reaction is quenched by adding 0.5 mL of oleic acid. The flask is cooled down to room temperature. The cleaning procedure is the same as before. Particles are stored in fresh hexane. The optical spectrum shows a first excitonic peak at 460 nm, see Figure S1 in the Supporting Information (SI).

NPL Synthesis CdTe 500. The procedure follows the one described by Pedetti et al. in ref 36. In a first step cadmium propanoate (Cd(Prop)₂) is prepared by mixing 1.036 g of CdO in 10 mL of propionic acid under Ar for 1 h. Then the flask is opened to air, and the temperature rises to 140 °C until the volume gets reduced by a factor of 2. The whitish solution is precipitated by addition of acetone. After centrifugation, the solid is dried under vacuum for 24 h. In the glovebox, 1 M TOPTe is prepared by stirring 2.55 g of Te pellets in 20 mL of TOP for 4 days at room temperature. In a three-neck flask 0.13 g of Cd(Prop)₂, 160 μL of oleic acid, and 10 mL ODE are degassed for 90 min at 95 °C. Then the atmosphere is switched to Ar, and the temperature rises to 210 °C. Then 0.2 mL of 1 M TOPTe is quickly injected into the flask. After 20 min the reaction is quenched by adding 1 mL of oleic acid and cooled down to room temperature. The cleaning process is done by adding ethanol to precipitate the CdTe platelets. The solid obtained after centrifugation is redispersed in hexane. This procedure is repeated three times. The optical spectrum shows a first excitonic peak at 500 nm, see Figure S2 in the SI.

Setup for Electrophoresis. For the electrophoretic deposition, a Spellman high-voltage DC supply is used as the voltage source. For selective cleaning we use two copper electrodes (5 cm long and spaced by 3 mm). For film deposition we used fluorine-doped tin oxide-coated glass slides as a conductive substrate, see Figure 1b. A U-shaped copper wire is used as the positive electrode, and an aluminum grid is added for a better homogeneity of the electric field. We apply bias in the 200 V to 2 kV range which typically corresponds to an electric field of some $\text{kV}\cdot\text{cm}^{-1}$. It is worth mentioning that the nanoparticles are only deposited on the positive electrodes and no significant material deposition is observed on the negative electrodes.

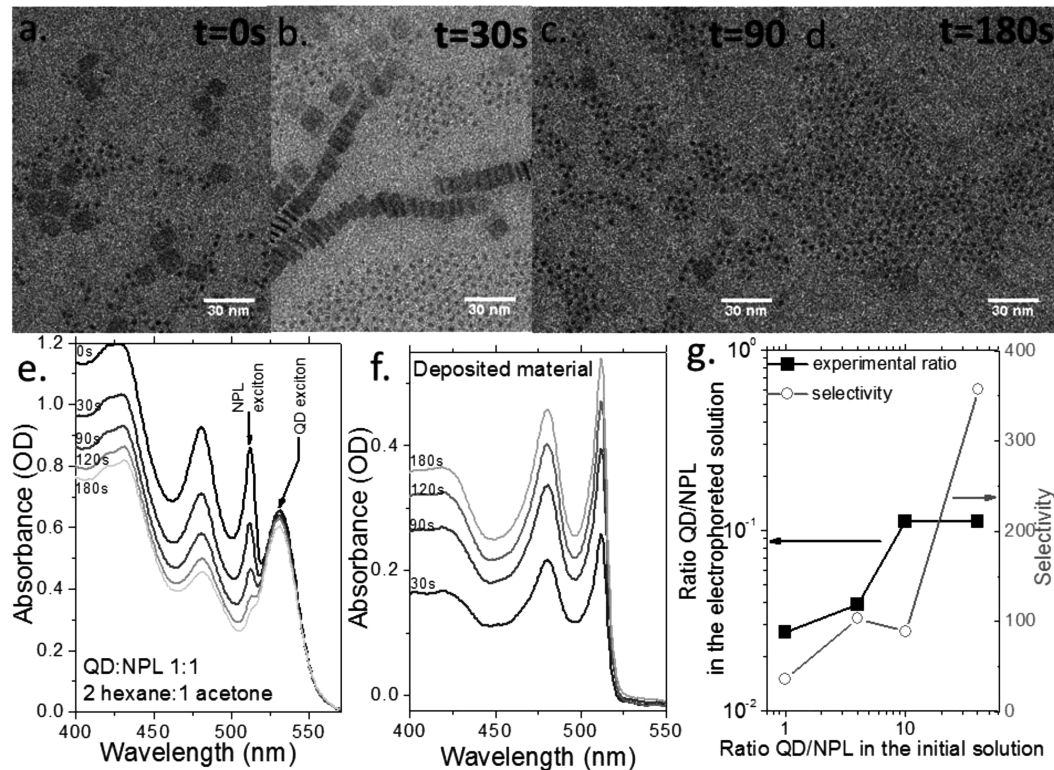


Figure 4. (a–d) TEM images of mixtures initially made of small CdSe QDs and CdSe NPLs at different times of the electrophoresis. The applied bias is 400 V. The solvent is made of hexane (66%) and acetone (33%). (e and f) Absorption spectra made at different times, respectively, from a mixture initially made of small CdSe QDs and CdSe NPLs and from the redispersed material. (g) Evolution of the ratio of QDs over NPL population (measured by the ratio of the optical density at the exciton peak) for the electrophoresed material (redispersed in hexane) as a function of the ratio of QDs and NPLs in the initial solution. The selectivity of the process is also plotted. The solvent is hexane/acetone 50:50. The applied bias is 400 V.

Characterization Device. Absorption spectra are acquired using a Cary 5E UV-visible spectrometer. Transmission electron microscopy images are obtained on a JEOL 2010 microscope, while scanning electron microscopy images are obtained from an FEI Magellan. Thickness measurements are made using an optical profilometer (Fogale Nanotech). Dynamic light scattering (DLS) has been obtained using an ALV goniometer (ALV/CGS3), while ζ -potential measurements are conducted on a Malvern zetasizer nanoseries.

RESULTS AND DISCUSSION

Kinetic Studies of the Electrophoretic Deposition. The first motivation of this work is the use of electrophoresis as a scalable and selective process for the cleaning of NPLs. The achievement of selectivity will be based on the difference of electrophoretic mobility of the NPLs compared to that of the other present species. As a first step we consequently conduct a kinetic study of the ED where pure populations of nanocrystals are used. We tested three populations of CdSe-based particles: NPLs, as well as small (3 nm) and large (6 nm) spherical quantum dots, see Figure 2a,b,d,e,g, and h for TEM and absorption spectra. In particular, the small QDs have been chosen as a model system of the side product resulting from the NPL synthesis, see Figure 1a.

The kinetic study of the ED is processed by dipping two copper electrodes in a solution of nanoparticles. The solvent is either hexane only or a mixture of hexane and acetone. The applied voltage is typically 400 V for a 5 mm spacing of the electrodes (equivalent electric field of $0.8 \text{ kV}\cdot\text{cm}^{-1}$). We only observe nanoparticle deposition on the positive electrodes. By

following the amount of deposited material in the early stages of the ED a linear dependence can be seen of the amount of deposited material with time and concentration, see Figure 3a and b. On the other hand, the dynamic of deposition is strongly dependent on the presence of polar solvent, see Figure 2c and Figure 3c. The exponential fit of the decay of the absorbance during the ED is 7.6 h in pure hexane and is reduced to less than a minute in a 50:50 hexane/acetone mixture. The role of the polar solvent is not completely elucidated, but it is clear that its presence (i) tunes the dielectric constant of the medium, (ii) favors the presence of ions, in particular the dissociation of the carboxylic acid into carboxylate, (iii) and leads to some aggregation of the nanoparticles as confirmed by the size change observed by the dynamic light-scattering measurement; see Figure S3 in the SI. At low acetone concentration the film thickness slowly increases due to the rise of the dielectric constant of the solvent. Above 15% of acetone the slope gets steeper which is related to the aggregation of the NPL.

We can relate the ED time constant to the electrophoretic mobility using the relation $(1/\tau) = ((\mu \cdot A \cdot E)/(V))$, where A is the area of the electrodes, E the electric field between the electrodes, and V is the volume of the solution. We estimate that the mobility is of the order of $1 \times 10^{-4} \text{ cm}^2 \text{ V}^{-1} \text{ s}^{-1}$ for the NPLs and large QDs in the presence of nonsolvent (50:50 hexane/acetone mixture) while a value of $5 \times 10^{-7} \text{ cm}^2 \text{ V}^{-1} \text{ s}^{-1}$ is obtained for the small QDs, in the same solvent. These estimations of the mobility are further confirmed within a decade while performing direct measurement of mobility using a ζ -meter, see Table SI in the SI. The limited quantitative difference very likely results from the

electric field dependence of mobility which is much higher in our setup compared to the one applied in the ζ -meter.

Our process is an electrophoretic deposition, performed with DC bias, and not a dielectrophoretic deposition³¹ that requires alternating current. The selection process is thus related to the charge of the nanoparticles and not to their polarization. To be more precise, in a permanent electric field, the mobility, μ , of nanoparticles with diameter a and a ζ -potential, ζ , in a solution of dielectric constant, ϵ , and viscosity, η , is given by the following equation:³² $\mu = ((2\epsilon)/(3\eta) \cdot \zeta f(a/\lambda_D))$, where f is the Henry's function³⁷ which depends on a the diameter of the nanoparticles and on λ_D , the Debye length. For a given solvent, the mobility of the nanoparticles, and thus the selectivity of the ED, depends on the particles' charge but also on the Henry's function. Since f ranges between 1 and 1.5 while the ratio a/λ_D is tuned, it is clear that the large change of mobility between big and small QD mostly results from a change of ζ value. The direct measurement of the ζ -potential using a ζ -meter confirms that, indeed, all particles have a slightly negative ζ -potential ranging from -10 mV for NPLs to -2 mV for small QDs, see Figure S3d and Table SI in the SI.

Electrophoresis of a Mixture. As a next step toward the selective cleaning of NPLs, we perform the ED process on a mixture of NPLs and small QDs, which again have their size fitting with the side product obtained during the NPL synthesis. We start by a 1:1 (in absorbance) NPL:QD mixture. A TEM image of the mixture is given in Figure 4a. The absorption spectrum (Figure 4e) of the solution in particular displays two distinct features related to the QDs (first absorption peak at 550 nm) and to the NPLs (first absorption peak at 510 nm). We follow the ED process by TEM imaging and optical absorption, see Figure 4a–e and Figure S4 in the SI. As the ED occurs, the peak related to the NPLs decreases in magnitude, while the one related to the QDs is barely affected. This is consistent with the fact that the NPLs aggregate on the electrodes and little by little are removed from the initial mixture. This speculation is confirmed by redispersing the deposited material in pure hexane. The yield of the deposition is high (>95%) (see Figure 4e and f) and has been conducted successfully up to gram-scale synthesis. The optical absorption of the deposited material, see Figure 4f, only shows the peaks related to NPLs. Moreover the magnitude of the first absorption peak is consistent with a full extraction of the NPLs from the initial mixture. We thus demonstrate that the ED can be used as a selective method to sort nanoparticles. We then tune the NPL:QD ratio and follow this ratio for the deposited material, see Figure 4g. The selectivity of the method is still observable even when NPL are introduced in minor quantity. Defining a selectivity as $S = (((\text{amount of NPLs})/(\text{amount of QDs}))_{\text{deposited}})/((\text{amount of NPLs})/(\text{amount of QDs}))_{\text{initial}})$, we obtain a value for S as high as 400, consistent with the ratio of the deposition time observed in Figure 2.

We have also tested the ability to separate NPLs from QDs directly after the synthesis. In this case, the spherical QDs are a byproduct of the reaction performed to obtain a majority of NPLs. The reaction mixture may also contain unreacted precursors, excess ligands, and a mixture of nonpolar solvents. In spite of this complexity we have been able to obtain a pure deposition of NPLs, see Figure 1a. The fact that this method can be performed on the crude mixture of NPL synthesis is very promising to achieve upscaling of the NPL synthesis. The NPLs that are selected using ED remain photoluminescent, see Figure S5 in the SI. However, compared to the NPLs cleaned with the usual precipitation method we observe a loss of the PL signal and

an increase of the deep trap emission. We attribute these observations to the fact that the ED process is non-neutral toward the capping ligands and probably removes them from the surface of the nanoparticles, leaving the surface charged and thus raising the absolute ζ -potential. This speculation is confirmed by the drop of the PL efficiency and the shorter deposition time while cycling the electrophoresis step, see Figure S5 in the SI.

Electrophoresis of NPLs with different thicknesses is also possible, but it is not very clear whether the difference results from a difference in thickness or in lateral extension while doing the experiment with CdSe core only. Indeed NPL 510 typically have a 4 monolayers thickness with a lateral size of 10 nm \times 40 nm (see Figure 2a) while NPL 460 have a 3 monolayers thickness but a lateral size of 100 nm (see Figure S1 in the SI). Consequently the NPL 460 are not colloidally stable and are deposited much faster by electrophoresis. In order to check the possibility to use electrophoresis to sort NPLs of different thicknesses we grow a CdS shell on CdSe NPL³⁸ and we obtain NPL with different thicknesses and similar lateral sizes. It appears that the thinner NPL tend to be deposited faster, see Figure S6 in the SI.

Phase Diagram for the Deposition of a QD:NPL Mixture. In conclusion, for a given solvent, the difference in mobility between nanoparticles (and thus the selectivity during the ED process) depends on the product $\zeta f(a/\lambda_D)$ where ζ gives the main modulation. The experiments we have performed with different types of nanoparticles and different solvents can be partially summarized in the phase diagram presented in Figure 5.

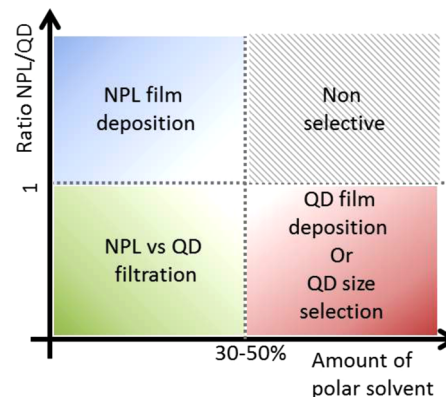


Figure 5. Phase diagram of the possible applications for electrophoresis of a NPL and QD mixture as a function of polar solvent amount and ratio of NPL vs QD.

When a mixture of QDs and NPLs is electrodeposited, three different regimes can be identified. At a low ratio of NPLs/QDs, and a low amount of polar solvent, efficient selection of NPLs vs QDs can be achieved. At high ratio of NPLs, homogeneous deposition of NPL films on large area can be rapidly obtained. When mostly spherical QDs are present in the solution, rapid ED of QDs can be performed when the solvent is highly polar. When the polar solvent is absent, QD size selection can be performed, but at the price of long deposition time.

Electrophoresis for Film Deposition of NPL. The use of ED to obtain films made of spherical QDs and nanorod-shaped materials have already been documented.^{16–20} In the following we test the potential of NPL ED to achieve thick film deposition (thickness of the order of 1 μm).

In Figure 6a, we show a film obtained with the ED of 40 nm \times 10 nm of CdSe NPLs on a substrate with centimeter scale. The

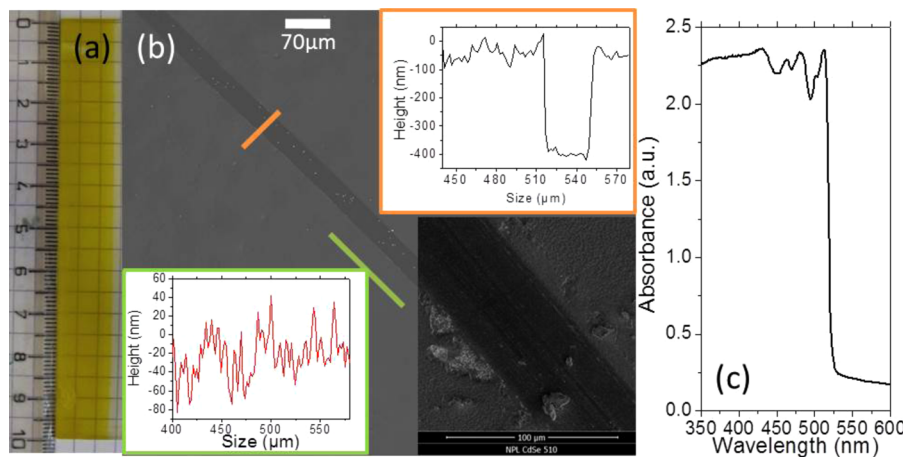


Figure 6. (a) Image of an electrophoresed film of NPLs, the scale bar is in cm. (b) SEM image of an electrophoresed (and scratched) film of NPLs. Some thickness and roughness measurement are added. The highlighted profiles correspond to the two lines on the image. The inset is an SEM picture around the groove. (c) Absorption spectrum of a film of NPL made of a layer of CdSe NPL 460, CdSe NPL 510, and CdTe NPL 500.

quality of the film is probed using a profilometer and scanning electron microscopy imaging. The typical roughness of the film is around 40–60 nm, see Figure 6b and its insets. This value is a trade-off with the deposition time. Smoother films can be achieved at the price of a longer deposition time. We also use ED to grow a multilayer system made of three different materials: CdSe NPL 460, CdSe NPL 510, and CdTe NPL 500. By adjusting the thickness of each layer we have been able to achieve a high pass filter (in wavelength) with a sharp transition due to the narrow transition of the NPL and an almost flat response on the absorbing side, see Figure 6c.

■ CONCLUSION

We demonstrate that ED can be used as a selective method to sort nanoparticles as a function of their shape and size. Moreover ED can be used to sort complex mixtures such as the one obtained at the end of a colloidal synthesis. Compared to other existing preparative methods, ED offers an easier path for the post-sorting use of the nanoparticles. The surface charge is the main parameter driving the selectivity of the ED, far above the size. A phase diagram as a function of the ratio of nonsolvent and ratio of the nanoparticles present describing the application of ED is also proposed. Finally we also point out the strong potential of ED for large-scale and homogeneous film deposition. Possible application as a narrow cutoff wavelength filter is also demonstrated.

■ ASSOCIATED CONTENT

Supporting Information

Details about the precursor and the nanoparticles synthesis. DLS and ζ -potential measurement. The effect of the ED on the PL. This material is available free of charge via the Internet at <http://pubs.acs.org>.

■ AUTHOR INFORMATION

Corresponding Author

*E-mail: benoit.dubertret@espci.fr

Notes

The authors declare no competing financial interest.

■ ACKNOWLEDGMENTS

We are grateful to X. Xu for performing the TEM measurements. B.D. thanks the ANR agency for funding. This work has been supported by the Region Ile-de-France in the framework of DIM Nano-K.

■ REFERENCES

- (1) Reiss, P.; Protiere, M.; Li, L. *Small* **2009**, *5*, 154–168.
- (2) Murray, C. B.; Norris, D. J.; Bawendi, M. G. *J. Am. Chem. Soc.* **1993**, *115*, 8706–8715.
- (3) Yin, Y.; Alivisatos, A. P. *Nature* **2005**, *437*, 664–670.
- (4) Morris-Cohen, A. J.; Malicki, M.; Peterson, M. D.; Slavin, J. W. J.; Weiss, E. A. *Chem. Mater.* **2013**, *25*, 1155–1165.
- (5) Chemseddine, A.; Weller, H. *Bunsen-Ges.* **1993**, *97*, 636–638.
- (6) Arnold, M. S.; Green, A. A.; Hulvat, J. F.; Stupp, S. I.; Hersam, M. C. *Nat. Nanotechnol.* **2006**, *1*, 60–65.
- (7) Stürzl, N.; Hennrich, F.; Lebedkin, S.; Kappes, M. M. *J. Phys. Chem. C* **2009**, *113*, 14628–14632.
- (8) Mastronardi, M. L.; Hennrich, F.; Henderson, E. J.; Maier-Flaig, F.; Blum, C.; Reichenbach, J.; Lemmer, U.; Kubel, C.; Wang, D.; Kappes, M. M.; Ozin, G. A. *J. Am. Chem. Soc.* **2011**, *133*, 11928–11931.
- (9) Fischer, C. H.; Weller, H.; Katsikas, L.; Henglein. *Langmuir* **1989**, *5*, 429–432.
- (10) Fischer, C. H.; Weller, H.; Fojtik, A.; Lumepereira, C.; Janata, E.; Henglein, A. *Ber. Bunsen-Ges.* **1986**, *90*, 46–49.
- (11) Shen, Y.; Gee, M. Y.; Tan, R.; Pellechia, P. J.; Greystak, A. B. *Chem. Mater.* **2013**, *25*, 2838–2848.
- (12) Pinaud, F.; King, D.; Moore, H. P.; Weiss, S. *J. Am. Chem. Soc.* **2004**, *126*, 6115–6123.
- (13) Sperling, R. A.; Liedl, T.; Duhr, S.; Kudera, S.; Zanella, M.; Lin, C. A. J.; Chang, W. H.; Braun, D.; Parak, W. J.; Size, J. *J. Phys. Chem. C* **2007**, *111*, 11552–11559.
- (14) Eychmuller, A.; Katsikas, L.; Weller, H. *Langmuir* **1990**, *6*, 1605–1608.
- (15) Mamedova, N. N.; Kotov, N. A.; Rogach, A. L.; Studer, J. *Nano Lett.* **2001**, *1*, 281–286.
- (16) Islam, M. A.; Herman, I. P. *Appl. Phys. Lett.* **2002**, *80*, 3823–3825.
- (17) Ahmed, S.; Ryan, K. M. *Adv. Mater.* **2008**, *20*, 4745–4750.
- (18) Song, K. W.; Costi, R.; Bulovic, V. *Adv. Mater.* **2013**, *25*, 1420–1423.
- (19) Benehkohal, N. P.; Gonzalez-Pedro, V.; Boix, P. P.; Chavhan, S.; Tena-Zaera, R.; Demopoulos, G. P.; Mora-Sero, I. *J. Phys. Chem. C* **2012**, *116*, 16391–16397.
- (20) Santra, P. K.; Kamat, P. V. *J. Am. Chem. Soc.* **2013**, *135*, 877–885.

- (21) Bass, J. D.; Ai, X.; Bagabas, A.; Rice, P. M.; Topuria, T.; Scott, J. C.; Alharbi, F. H.; Kim, H. C.; Song, Q.; Miller, R. D. *Angew. Chem., Int. Ed.* **2011**, *50*, 6538–6542.
- (22) Singh, A.; English, N. J.; Ryan, K. M. *J. Phys. Chem. B* **2013**, *117*, 1608–1615.
- (23) Dickerson, J. H., Electrophoretic Deposition of Nanocrystals in Non-polar Solvents. In *Electrophoretic Deposition of Nanomaterials*; Springer: New York, 2012, 131–155.
- (24) Ithurria, S.; Dubertret, B. *J. Am. Chem. Soc.* **2008**, *130*, 16504–16505.
- (25) Ithurria, S.; Tessier, M. D.; Mahler, B.; Lobo, R. P. S. M.; Dubertret, B.; Efros, A. L. *Nat. Mater.* **2011**, *10*, 936–941.
- (26) Son, J. S.; Wen, X. D.; Joo, J.; Chae, J.; Baek, S. I.; Park, K.; Kim, J. H.; An, K.; Yu, J. H.; Kwon, S. G.; Choi, S. H.; Wang, Z. W.; Kim, Y. W.; Kuk, Y.; Hoffmann, R.; Hyeon, T. *Angew. Chem., Int. Ed.* **2009**, *48*, 6861–6864.
- (27) Joo, J.; Son, J. S.; Kwon, S. G.; Yu, J. H.; Hyeon, T. *J. Am. Chem. Soc.* **2006**, *128*, 5632–5633.
- (28) Liu, Y. H.; Wayman, V. L.; Gibbons, P. C.; Loomis, R. A.; Buhr, W. E. *Nano Lett.* **2010**, *10*, 352–357.
- (29) Li, Z.; Peng, X. G. *J. Am. Chem. Soc.* **2011**, *133*, 6578–6586.
- (30) Bouet, C.; Mahler, B.; Nadal, B.; Abecassis, B.; Tessier, M. D.; Ithurria, S.; Xu, X. Z.; Dubertret, B. *Chem. Mater.* **2013**, *25*, 639–645.
- (31) Tessier, M. D.; Javaux, C.; Maksimovic, I.; Loriette, V.; Dubertret, B. *ACS Nano* **2012**, *6*, 6751–6758.
- (32) Lhuillier, E.; Pedetti, S.; Ithurria, S.; Heuclin, H.; Nadal, B.; Robin, A.; Patriarche, G.; Lequeux, N.; Dubertret, B. *ACS Nano* **2014**, *8*, 3813–3820.
- (33) Lhuillier, E.; Robin, A.; Ithurria, S.; Aubin, H.; Dubertret, B. *Nano Lett.* **2014**, *14*, 2715–2719.
- (34) Yang, Y. A.; Wu, H.; Williams, K. R.; Cao, Y. C. *Angew. Chem.* **2005**, *117*, 6870–6873.
- (35) Bouet, C.; Mahler, B.; Nadal, B.; Abecassis, B.; Tessier, M. D.; Ithurria, S.; Xu, X.; Dubertret, B. *Chem. Mater.* **2013**, *25*, 639–645.
- (36) Pedetti, S.; Nadal, B.; Lhuillier, E.; Mahler, B.; Bouet, C.; Abécassis, B.; Xu, X.; Dubertret, B. *Chem. Mater.* **2013**, *25*, 2455–2462.
- (37) Henry, D. C. *Proc. R. Soc. London, Ser. A* **1931**, *133*, 106–129.
- (38) Ithurria, S.; Talapin, D. V. *J. Am. Chem. Soc.* **2012**, *134*, 18585–90.